Dyes and Pigments 91 (2011) 153–163

Contents lists available at ScienceDirect

Dyes and Pigments

journal homepage: www.elsevier.com/locate/dyepig

Water-soluble quaternized mercaptopyridine-substituted zinc-phthalocyanines: Synthesis, photophysical, photochemical and bovine serum albumin binding properties

Mahmut Durmuş [a,*], Hanifi Yaman [a], Cem Göl [a], Vefa Ahsen [a,b], Tebello Nyokong [c]

[a] Gebze Institute of Technology, Department of Chemistry, PO Box 141, Gebze, 41400 Kocaeli, Turkey
[b] TUBITAK-Marmara Research Center, Materials Institute, PO Box 21, Gebze, 41470 Kocaeli, Turkey
[c] Department of Chemistry, Rhodes University, Grahamstown 6140, South Africa

ARTICLE INFO

Article history:
Received 3 January 2011
Received in revised form
4 February 2011
Accepted 7 February 2011
Available online 8 March 2011

Keywords:
Phthalocyanine
Quaternization
Water soluble
Photosensitizer
Bovine serum albumin
Photodynamic therapy

ABSTRACT

The synthesis and characterization of the new zinc phthalocyanine derivatives, tetra- (non-peripheral, **5**) and octa-(peripheral, **6)** substituted with 2-mercaptopyridine and their respective quaternized derivatives (**8** and **9**) are reported. Photochemical and photophysical properties of the new complexes are compared with those of the previously reported peripherally tetra-substituted complexes **7** and **10**. The quaternized compounds exhibit excellent solubility in water, making them potential photosensitizers for use in photodynamic therapy (PDT) of cancer. Spectroscopic, aggregation, photophysical and photochemical properties of these complexes are also investigated and compared. Photophysical (fluorescence quantum yields and lifetimes) and photochemical (singlet oxygen and photodegradation quantum yield) properties of these phthalocyanine photosensitizers are very important for the assessment of these complexes as PDT agents. In this study, the effects of the position of the substituents and quaternization of the substituents on the photophysical and photochemical parameters of the zinc phthalocyanines are also reported. This study also showed that the water-soluble quaternized zinc phthalocyanines strongly bind to blood plasma proteins such as bovine serum albumin (BSA).

1. Introduction

Phthalocyanines (Pcs) are remarkable macrocyclic compounds having magnificent physical and chemical properties [1]. Metallophthalocyanines (MPc) have been investigated in detail for many years due to their wide applications in many fields, mostly in terms of their uses as blue-green dyes and catalysts [2,3]. They have also found different applications in many fields ranging from industrial [4], technological [5,6] to medical [7,8]. Most metal ions can be engaged in the Pc macrocyle's cavity; therefore, a large number of different MPc complexes have been synthesized. When the central metal is diamagnetic and non-transitional, MPc derivatives are photoactive and may be employed in photosensitization [9,10]. In this regard, it is worth emphasizing the Pcs' application as photosensitizers in the photodynamic therapy (PDT) of tumours. High triplet state quantum yields and long triplet lifetimes are required for efficient sensitization by MPc complexes. The photophysical properties of the Pc dyes are strongly influenced by the presence and nature of the central metal ion. MPcs containing transition metals give short triplet lifetimes. Closed shell and diamagnetic ions, for example Zn^{2+}, Ga^{3+} and Si^{4+}, give Pc complexes excellent properties such as high triplet yields and long lifetimes [11–13]. ZnPcs in particular have been extensively studied because of d^{10} configuration of the central Zn^{2+} ion results in optical spectra that are not complicated by additional bands, as in transition-metal Pc complexes. ZnPcs have intensive red-visible region absorption and high singlet and triplet yields, making them valuable photosensitizers for PDT applications.

In PDT applications, the drug is injected into the patient's blood stream, and since the blood itself is a hydrophilic system, water solubility plays a very important role for a potential photosensitizer in PDT [14–17]. The advantages of MPcs bearing cationic substituents over those with neutral and anionic substituents are numerous [18], for examples: (i) they are able to improve water solubility and prevent aggregation [19]; aggregation seriously compromises the PDT value of the photosensitizer, (ii) they are more efficient as PDT agents [20] and also improve cell uptake [21], (iii) they are selectively localized in the cell mitochondria and cause apoptosis [22].

* Corresponding author. Tel.: +90 262 6053075; fax: +90 262 6053101.
E-mail address: durmus@gyte.edu.tr (M. Durmuş).

0143-7208/$ – see front matter © 2011 Elsevier Ltd. All rights reserved.
doi:10.1016/j.dyepig.2011.02.007

Thiol-substituted MPc complexes are known to absorb light at longer wavelengths (>700 nm) [23–26] and to exhibit good spectroscopic and photochemical properties. Therefore these complexes have a very useful feature for applications in optoelectronics, near-IR devices and PDT.

The aim of our ongoing research is to synthesise water-soluble zinc Pc complexes as potential PDT agents. Herein, we report on the synthesis, characterization and spectroscopic behavior as well as photophysical (fluorescence quantum yields and lifetimes) and photochemical (singlet oxygen and photodegradation quantum yields) properties of zinc Pc complexes tetra-substituted at the non-peripheral (**5**), and octasubstituted at the peripheral (**6**) positions with a 2-mercaptopyridine group (Scheme 1) and their quaternized (**8** for tetra-non-peripheral, and **9** for octa-peripheral position) complexes (Scheme 2). The photophysical and photochemical properties of these complexes are compared with those of the previously reported tetra substituted complexes **7** and **10**.

Bovine serum albumin (BSA) and human serum albumin (HSA) are major plasma proteins, which contribute significantly to physiological functions and display effective drug delivery roles [27,28], hence the investigation of binding of drugs with albumin is of interest. A spectroscopic investigation of the binding of the water-soluble zinc Pc complexes (**8**, **9** and **10**) to BSA is also presented in this work.

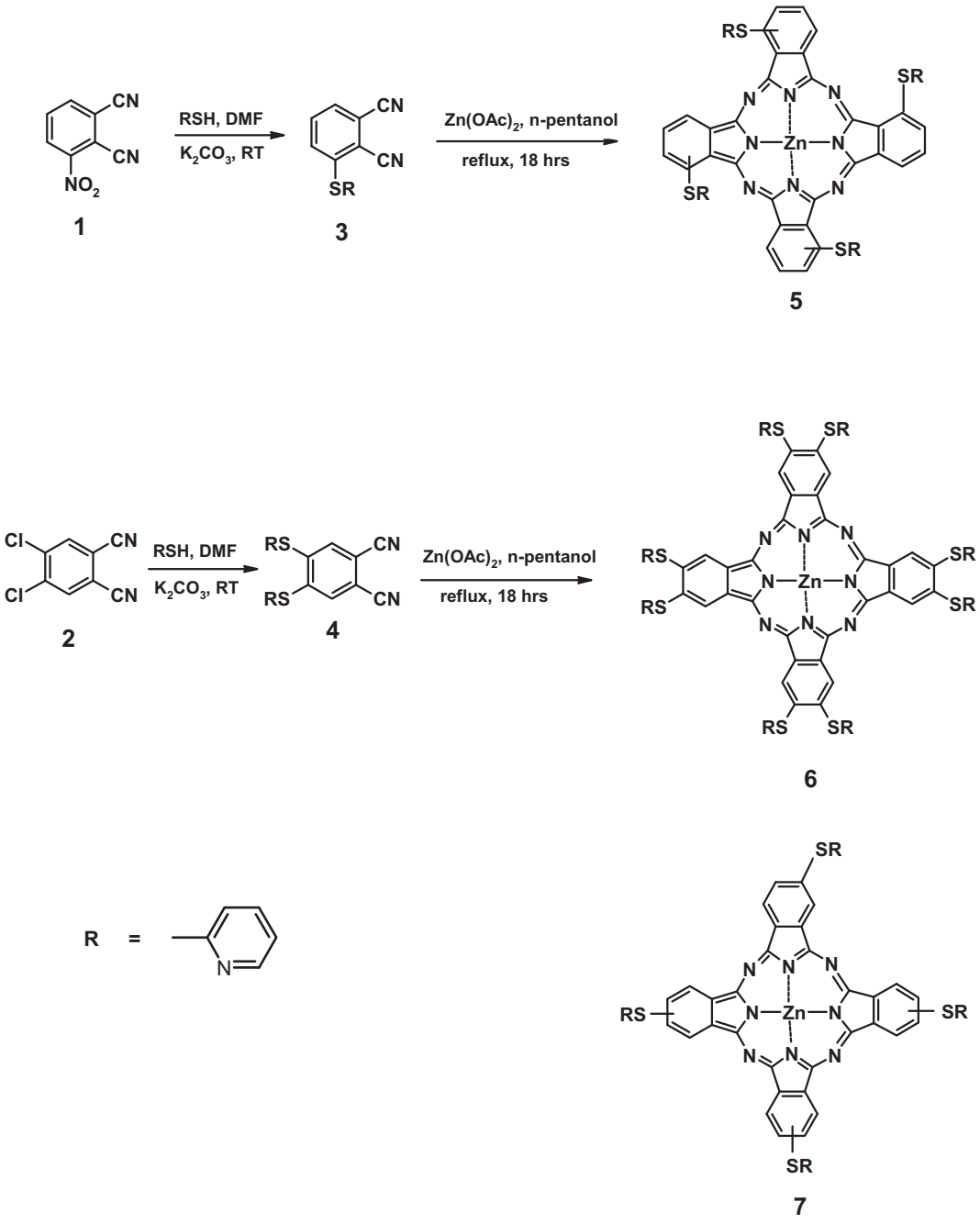

Scheme 1. Synthesis of tetra- and octa-2-mercaptopyridine substituted zinc phthalocyanine complexes. The synthesis of complex **7** has been reported before [33].

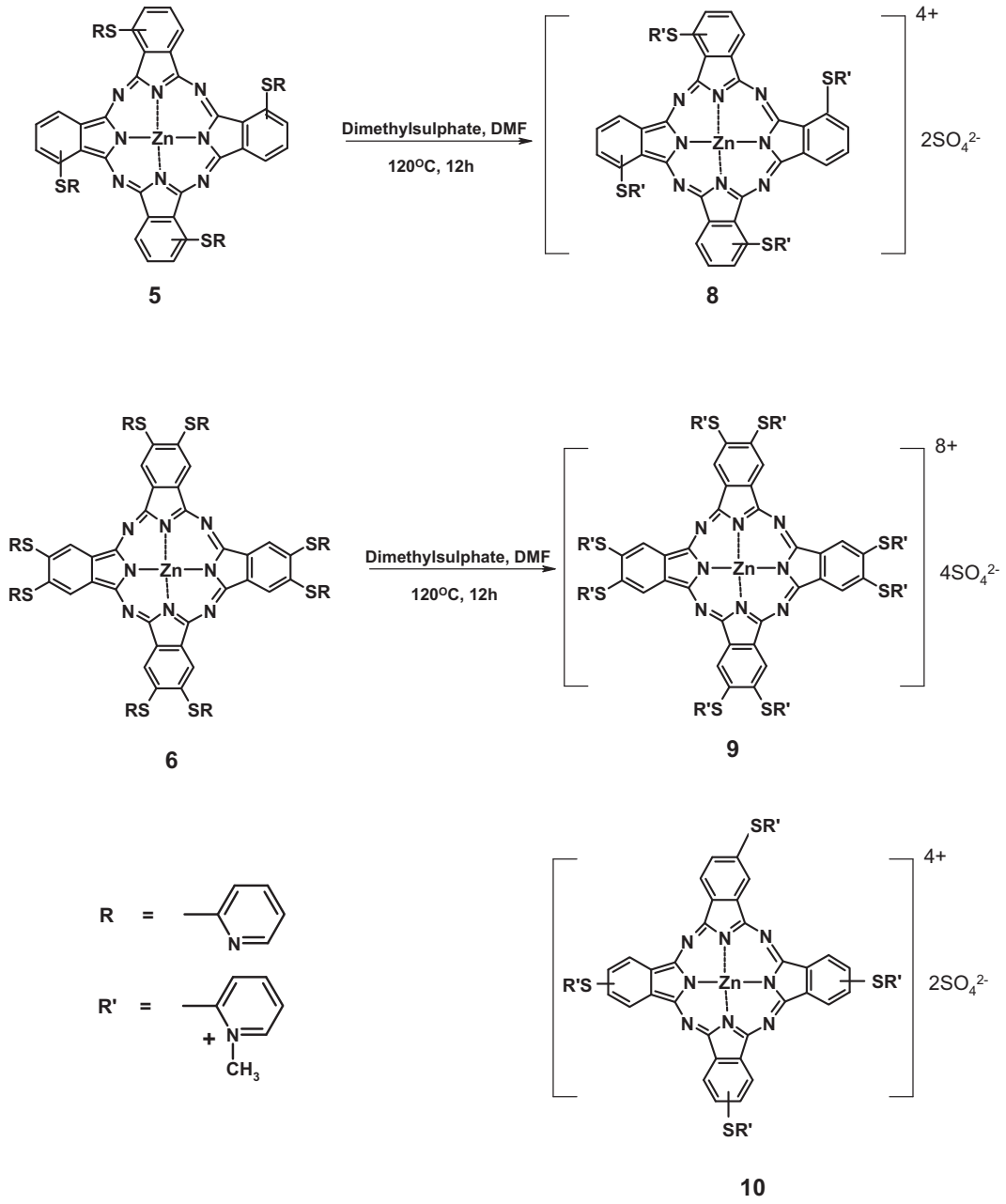

Scheme 2. Synthesis of quaternized tetra- and octa-2-mercaptopyridine substituted zinc phthalocyanine complexes. The synthesis of complex 10 has been reported before [33].

2. Experimental section

2.1. Materials

Quinoline, dimethylsulphoxide (DMSO), methanol, n-hexane, chloroform ($CHCl_3$), dichloromethane (DCM), tetrahydrofuran (THF), acetone, ethanol and dimethylformamide (DMF) were dried as described in Perrin and Armarego [29] before use. Unsubstituted zinc phthalocyanine, zinc (II) acetate, K_2CO_3, dimethylsulphate (DMS) were purchased from Aldrich. 2-Mercaptopyridine was purchased from Fluka. 3-Nitrophthalonitrile (**1**) [30], 4,5-dichlorophthalonitrile (**2**) [31], 3-(2-mercaptopyridine)phthalonitrile (**3**) [32], 2,(3)-tetra-(2-mercaptopyridine) phthalocyaninatozinc (II) (**7**) [33] and quaternized 2,(3)-tetra-(2-mercaptopyridine)phthalocyaninato zinc (II) (**10**) [33] were synthesized and purified according to literature procedures. $ZnPcS_{mix}$ containing a mixture of differently sulfonated derivatives was synthesized as reported before [34].

2.2. Equipment

Absorption spectra in the UV–visible region were recorded with a Shimadzu 2001 UV spectrophotometer. Fluorescence excitation and emission spectra were recorded on a Varian Eclipse spectrofluorometer using 1 cm pathlength cuvettes at room temperature. IR spectra (KBr pellets) were recorded on a Bio-Rad FTS 175C FTIR spectrometer. The mass spectra were acquired on a Bruker Daltonics (Bremen, Germany) MicrOTOF mass spectrometer equipped with an electronspray ionization (ESI) source. The instrument was operated in positive ion mode using a *m/z* range of 50–3000. The capillary voltage of the ion source was set at 6000 V and the

capillary exit at 190 V. The nebulizer gas flow was 1 bar and drying gas flow 8 cm^3/min. The drying temperature was set at 200 °C for non-ionized complexes (**5**–**7**) and positive ion and linear mode MALDI-MS spectrum of quaternized complex (**8**) was obtained in 3,5-dimethoxy-4-hydroxycinnamic acid as MALDI matrix using nitrogen laser accumulating 50 laser shots using by Bruker Microflex LT MALDI-TOF mass spectrometer. ^{1}H spectra were recorded in $CDCl_3$ for phthalonitrile (**4**) and DMSO-d_6 solutions for phthalocyanine complexes (**5**,**6**,**8**,**9**) on a Varian 500 MHz spectrometer. Elemental analyses were obtained with a Thermo Finnigan Flash 1112 Instrument.

Photo-irradiations were done using a General Electric quartz line lamp (300W). A 600 nm glass cut off filter (Schott) and a water filter were used to filter off ultraviolet and infrared radiations respectively. An interference filter (Intor, 670 nm with a band width of 40 nm) was additionally placed in the light path before the sample. Light intensities were measured with a POWER MAX5100 (Molelectron detector incorporated) power meter.

2.3. Photophysical parameters

2.3.1. Fluorescence quantum yields and lifetimes

Fluorescence quantum yields (Φ_F) were determined by the comparative method (Eq. (1)) [35,36],

$$\Phi_F = \Phi_F(Std)\frac{F \cdot A_{Std} \cdot n^2}{F_{Std} \cdot A \cdot n_{Std}^2} \quad (1)$$

where F and F_{Std} are the areas under the fluorescence emission curves of the samples (**5**,**6** and **8**,**9**) and the standard, respectively. A and A_{Std} are the respective absorbances of the samples and standard at the excitation wavelengths, respectively. n and n_{Std} are the refractive indices of solvents used for the sample and standard, respectively. Unsubstituted ZnPc (in DMSO) ($\Phi_F = 0.20$) [37] was employed as the standard. The absorbance of the solutions at the excitation wavelength ranged between 0.04 and 0.05.

Natural radiative (τ_0) lifetimes were determined using PhotochemCAD program which uses the Strickler–Berg equation [38]. The fluorescence lifetimes (τ_F) were evaluated using Eq. (2).

$$\Phi_F = \frac{\tau_F}{\tau_0} \quad (2)$$

2.4. Photochemical parameters

2.4.1. Singlet oxygen quantum yields

Singlet oxygen quantum yield ($\Phi\Delta$) determinations were carried out using the experimental set-up described in literature [34,39,40]. Typically, a 3 cm^3 portion of the respective non-peripherally tetra- (**5**, **8**) and peripherally octa- (**6**,**9**) substituted zinc (II) phthalocyanine derivatives, (absorbance ~ 1 at the irradiation wavelength) containing the singlet oxygen quencher was irradiated in the Q band region with the photo-irradiation set-up described in references [34,39,40]. Singlet oxygen quantum yields (Φ_Δ) were determined in air using the relative method with ZnPc (in DMSO) or $ZnPcS_{mix}$ (in aqueous media) as references. DPBF and ADMA were used as chemical quenchers for singlet oxygen in DMSO and aqueous media, respectively. Eq. (3) was employed for the calculations:

$$\Phi_\Delta = \Phi_\Delta^{Std}\frac{R \cdot I_{abs}^{Std}}{R^{Std} \cdot I_{abs}} \quad (3)$$

where Φ_Δ^{Std} is the singlet oxygen quantum yields for the standard ZnPc ($\Phi_\Delta^{Std} = 0.67$ in DMSO) [41] and $ZnPcS_{mix}$ ($\Phi_\Delta^{Std} = 0.45$ in aqueous media) [42]. R and R_{Std} are the DPBF (or ADMA) photobleaching rates in the presence of the ZnPc derivatives and standards, respectively. I_{abs} and I_{abs}^{Std} are the rates of light absorption by ZnPc derivatives and standards, respectively. To avoid chain reactions induced by DPBF (or ADMA) in the presence of singlet oxygen [43], the concentration of quenchers (DPBF or ADMA) was lowered to ~3×10^{-5} M. Solutions of sensitizer containing DPBF (or ADMA) were prepared in the dark and irradiated in the Q band region using the set-up described above. DPBF degradation at 417 nm (in DMSO) and ADMA degradation at 380 nm (in water) were monitored. The light intensity 6.72×10^{15} photons s^{-1} cm^{-2} was used for Φ_Δ determinations.

2.4.2. Photodegradation quantum yields

Photodegradation quantum yield (Φ_d) determinations were carried out using the experimental set-up described in literature [34,39,40]. Photodegradation quantum yields were determined using Eq. (4),

$$\Phi_d = \frac{(C_0 - C_t) \cdot V \cdot N_A}{I_{abs} \cdot S \cdot t} \quad (4)$$

where C_0 and C_t are the samples (**5**–**7** and **8**–**10**) concentrations before and after irradiation respectively, V is the reaction volume, N_A is the Avogadro's constant, S is the irradiated cell area, t is the irradiation time and I_{abs} is the overlap integral of the radiation source light intensity and the absorption of the samples (**5**–**7** and **8**–**10**). A light intensity of 2.24×10^{16} photons s^{-1} cm^{-2} was employed for Φ_d determinations.

2.4.3. Binding studies of quaternized zinc phthalocyanine complexes to BSA

The binding properties of the water-soluble quaternized phthalocyanine complexes (**8**–**10**) to BSA were studied by spectrofluorometry at room temperature. An aqueous solution of BSA (fixed concentration) was titrated with varying concentrations of the respective samples (**8**–**10**) solutions in water. BSA was excited at 280 nm and fluorescence recorded between 290 and 500 nm. The steady diminution in BSA fluorescence with increase in quaternized cationic zinc Pc concentrations was noted and used in the determination of the binding constants and the number of binding sites on BSA, according to Eq. (5) [44–46].

$$\log\left[\frac{(F_0 - F)}{(F - F_\infty)}\right] = \log K_b + n\log[Pc] \quad (5)$$

where F_0 and F are the fluorescence intensities of BSA in the absence and presence of quaternized cationic Pc complexes (**8**–**10**) respectively; $F\infty$, the fluorescence intensity of BSA saturated with quaternized cationic Pc complexes; K_b, the binding constant; n, the number of binding sites on a BSA molecule; and [Pc] the concentration of quaternized cationic Pc complexes. Plots of $\log[(F_0 - F)/(F - F_\infty)]$ against log [Pc] would provide the values of n (from the slope) and K_b (from the intercept). The changes in BSA fluorescence intensity were related to quaternized cationic Pc concentrations by the Stern–Volmer relationship (Eq. (6)):

$$\frac{F_0^{BSA}}{F^{BSA}} = 1 + K_{SV}^{BSA}[Pc] \quad (6)$$

and K_{SV}^{BSA} is given by Eq. (7):

$$K_{SV}^{BSA} = k_q \tau_{F(BSA)} \quad (7)$$

where F_0^{BSA} and F^{BSA} are the fluorescence intensities of BSA in the absence and presence of quaternized cationic Pc complexes (**8**–**10**),

respectively. K_{SV}^{BSA} is the Stern–Volmer quenching constant; k_q is the bimolecular quenching constant and $\tau_{F(BSA)}$ is the fluorescence lifetime of BSA. $\tau_{F(BSA)}$ is known to be 10 ns [47–49], thus from the values of K_{SV}^{BSA} obtained from the plots of F_0^{BSA}/F^{BSA} versus [Pc], the value of k_q may be determined from Eq. (7).

2.5. Synthesis

2.5.1. 4,5-Bis-(2-mercaptopyridine)phthalonitrile (**4**, Scheme 1)

In a stream of nitrogen, 2-mercaptopyridine (6.74 g, 60.8 mmol) and 4,5-dichlorophthalonitrile (**2**) (6.00 g, 30.4 mmol) were dissolved in DMF (100 cm^3) and the mixture stirred at room temperature for 30 min. Thereafter, finely ground K_2CO_3 (15 g, 108 mmol) was added portion-wise over a period of 4 h and the reaction mixture left to stir for a further 12 h at room temperature. The mixture was added to water (100 cm^3) and stirred for 30 min. The resulting precipitate was filtered off, thoroughly washed with water, dried and recrystallised from chloroform/ethanol (1/4). M.p.: 220 °C Yield: 5.79 g (55%). IR [(KBr) ν_{max}/cm^{-1}]: 3037(Ar–CH), 2230 (C≡N), 1574 (C=C). ^1H NMR ($CDCl_3$): δ, ppm 8.55 (d, 2H, Pyridyl-H), 7.83 (s, 2H, Pc-H), 7.70 (t, 2H, Pyridyl-H), 7.38 (d, 2H, Pyridyl-H), 7.28 (t, 2H, Pyridyl-H). Calc. for $C_{18}H_{10}N_4S_2$: C 62.41, H 2.91, N 16.17; Found: C 62.20, H 2.80, N 16.17. MS (ESI-MS) *m/z*: Calc. 346; Found: 347.1 $[M + H]^+$.

2.5.2. 1,(4)-Tetrakis-(2-mercaptopyridine)phthalocyaninatozinc (II) (**5**, Scheme 1)

A mixture of anhydrous zinc (II) acetate (0.77 g, 4.22 mmol), 3-(2-mercaptopyridine)phthalonitrile (**3**) (1.0 g, 4.22 mmol), DBU (0.97 cm^3, 0.65 mmol) and 10 cm^3 dried n-hexanol was stirred at 160 °C for 12 h under nitrogen atmosphere. After cooling, the solution was dropped in the n-hexane. The green solid product was precipitated and collected by filtration and washed with n-hexane. The crude product was dissolved in chloroform and precipitated again by dropping in n-hexane. The green solid product was collected by filtration and washed with n-hexane. The green crude product was purified by passing through an alumina column with firstly ethyl acetate and then ethyl acetate/MeOH (5:1) elution. M.p. > 240^0C Yield: 0.13 g (12%). UV/Vis (DMSO): λ_{max} nm (log ϵ) 342 (4.81), 631 (4.58), 700 (5.29). IR [(KBr) ν_{max}/cm^{-1}]: 3045(Ar–CH), 1570(C=C), 1451, 1416, 1316, 1103, 895, 756, 741. ^1H NMR (DMSO-d_6): δ, ppm 9.32–9.10 (m, 4H, Pyridyl-H), 8.68–8.50 (m, 4H, Pyridyl-H), 8.11–7.68 (m, 16H, Pc-H and Pyridyl-H), 7.33–7.25 (m, 4H, Pyridyl-H). Calc. for $C_{52}H_{28}N_{12}S_4Zn$: C 61.56, H 2.78, N 16.57; Found: C 61.40, H 2.70 N 16.45. ESI-MS *m/z*: Calc. 1012; Found: 1013.2 $[M + H]^+$.

2.5.3. 2,3-Octakis-(2-mercaptopyridine)phthalocyaninato zinc (II) (**6**, Scheme 1)

Synthesis and purification was as outlined for **5** except 4,5-bis-(2-mercaptopyridine)phthalonitrile (**4**) instead of 3-(2-mercaptopyridine)phthalonitrile (**3**) was employed. The amounts of the reagents employed were: **4** (1.00 g, 2.9 mmol), anhydrous zinc (II) acetate (0.53 g, 2.9 mmol), DBU (0.67 cm^3, 0.45 mmol) in n-hexanol (5 cm^3). Yield: 0.11 g (10%). M.p. > 240^0C. Yield: 0.13 g (12%). UV/Vis (DMSO): λ_{max} nm (log ϵ) 373 (4.78), 638 (4.80), 667 (4.75), 707 (5.24). IR [(KBr) ν_{max}/cm^{-1}]: 3045(Ar–CH), 1574(C=C), 1451, 1416, 1281, 1119, 945, 760. ^1H NMR (DMSO-d_6): δ, ppm 9.12 (br, 8H, Pyridyl-H), 8.93 (br, 8H, Pc-H), 7.66 (br, 8H, Pyridyl-H), 7.30 (br, 8H, Pyridyl-H), 7.15 (br, 8H, Pyridyl-H), Calc. for $C_{72}H_{40}N_{16}S_8Zn$: C 59.59, H 2.78, N 15.44; Found: C 59.41, H 2.72 N 15.34. ESI-MS *m/z*: Calc. 1450; Found: 1451.2 $[M + H]^+$.

2.5.4. Quaternized 1,(4)-tetrakis-[(2-mercaptopyridine) phthalocyaninato] zinc (II) (**8**, Scheme 2)

Compound **5** (0.18 g, 0.177 mmol) was heated to 120 °C in freshly distilled DMF (5 cm^3) and excess dimethylsulphate (0.168 cm^3) was added dropwise. The mixture was stirred at 120 °C for 12h. After this time, the mixture was cooled to room temperature and the product was precipitated with hot acetone and collected by filtration. The green solid product was washed successively with hot ethyl acetate, chloroform, n-hexane, CCl_4 and diethyl ether. The resulting hygroscopic product was dried over phosphorous pentoxide. M.p. > 240 °C. Yield: 0.17 g (77%). UV/Vis (DMSO): λ_{max} nm (log ϵ) 327 (4.62), 627 (4.38), 691(5.02). IR [(KBr) ν_{max}/cm^{-1}]: 3041(Ar–CH), 2955 (CH), 1563(C=C), 1485, 1439, 1227(S=O), 1107(S=O), 586(S–O). ^1H NMR (DMSO-d_6): δ, ppm 9.74–6.91 (m, 28H, Pc-H and Pyridyl-H), 4.33 (d, 12H, CH_3). Calc. for $C_{56}H_{50}N_{12}O_{13}S_6Zn$ (+$5H_2O$): C 49.57, H 3.71, N 12.39; Found: C 50.13, H 3.27, N 12.87. MALDI-TOF-MS m/z: Calc. for $C_{56}H_{40}N_{12}O_8S_6Zn$, 1266; Found 1167 $[M - SO_4]^+$, 1073.6 $[M\text{-}2SO_4]^+$ 1042.1, $[M–2SO_4–2CH_3]^+$.

2.5.5. Quaternized 2,3-octakis-[(2-mercaptopyridine) phthalocyaninato] zinc (II) (**9**, Scheme 2)

Synthesis and purification was as outlined for **8** except compound **6** instead compound **5** was employed. The amounts of the reagents employed were: **6** (0.18 g, 0.124 mmol), excess dimethylsulphate (0.118 cm^3, 1.24 mmol) in DMF (5 cm^3). M.p. > 240 °C. Yield: 0.19 g (79%). UV/Vis (DMSO): λ_{max} nm (log ϵ) 377 (4.79), 639 (4.44), 704(4.90). IR [(KBr) ν_{max}/cm^{-1}]: 3056(Ar–CH), 2953 (CH), 1566(C=C), 1489, 1223(S=O), 1115(S=O), 586(S–O). ^1H NMR (DMSO-d_6): δ, ppm 10.13 (br, 4H, Pyridyl-H), 9.14 (s, 8H, Pc-H), 8.25 (br, 12H, Pyridyl-H), 7.91–7.88 (m, 16H, Pyridyl-H), 4.51 (s, 24H, CH_3). Calc. for $C_{80}H_{74}N_{16}O_{21}S_{12}Zn$ (+$5H_2O$): C 46.97, H 3.65, N 10.95; Found: C 47.34, H 3.98, N 11.42.

3. Results and discussion

3.1. Synthesis and characterization

Generally, substituted phthalocyanines are prepared by cyclotetramerization of substituted phthalonitriles or 1,3-diimino-1*H*-isoindoles. 2(3),9(10),16(17),23(24)-Tetra-substituted phthalocyanines can be synthesized from 4-substituted phthalonitriles while 1(4),8(11),15(18),22(25)-tetra-substituted phthalocyanines are obtained from 3-substituted analogues [50]. 2,3,9,10,16,17,23,24-Octa-substituted phthalocyanines can be synthesized from 4,5-disubstituted phthalonitriles. For tetra-substituted derivatives, a mixture of four possible structural isomers is obtained. In this study, synthesized tetra-substituted phthalocyanine compounds are obtained as isomer mixtures as expected. No attempt was made to separate the isomers of **5** and **8**.

The preparation of phthalocyanine complexes from the aromatic nitriles occurs under different reaction conditions. The synthesis of zinc phthalocyanine complexes (**5**,**6**) were achieved by treatment of phthalonitriles **3** and **4** with anhydrous zinc(II) acetate in dried n-hexanol (Scheme 1). Column chromatography with neutral alumina was employed to obtain the pure products from the reaction mixtures.

Quaternization of the zinc phthalocyanine complexes was achieved by reaction with excess dimethylsulphate (DMS) as quaternization agent in DMF at 120 °C. The yields of the products were 77% for **8** and 79% for **9**. After reaction with DMS, quaternized complexes are very soluble in water (Scheme 2).

Generally, phthalocyanine complexes are insoluble in most organic solvents; however introduction of substituents on the ring increases the solubility. All complexes (**5**–**7** and **8**–**10**) exhibited

excellent solubility in DMF and DMSO. Quaternized complexes (**8**–**10**) are soluble in water as well. The new compounds (**5**,**6**,**8** and **9**) were characterized by UV–vis, IR and NMR spectroscopies, mass spectra and elemental analysis. The analyses are consistent with the predicted structures as shown in the experimental section. The sharp peak in the IR spectra for the C≡N vibrations of phthalonitriles **3** and **4** at ~2230 cm^{-1} disappeared after conversion into zinc phthalocyanines, indicative of metallophthalocyanine formation. The characteristic vibrations corresponding to C=C groups at ~1570 cm^{-1}, and aromatic CH stretching at 3041–3056 cm^{-1} were observed for all complexes. Aliphatic CH stretches were observed at ~2950 cm^{-1} for quaternized complexes. S=O stretching at ~1220 and ~1110 cm^{-1}, S–O stretching at 586 cm^{-1} for quaternized complexes are indicative of quaternization formation.

The ^1H NMR spectra of tetra-substituted phthalocyanine derivatives (**5** and **8**) show complex patterns due to the mixed isomer character of these compounds. The octasubstituted complexes (**6** and **9**) show more resolved patterns due to presence of just one isomer. The complexes were found to be pure by ^1H NMR with all the substituents and ring protons observed in their respective regions. The resonances were observed as multiplets between 9.32 and 9.10 ppm, 8.68 and 8.50 ppm, 8.11 and 7.68 ppm, and 7.33 and 7.25 ppm integrating for 4, 4, 16, 4 protons each, making a total of 28 protons expected for both phthalocyanine ring and mercaptopyridine protons for **5**. For complex **6**, the resonances were observed as broad peaks at 9.12 ppm, 7.66 ppm, 7.30 ppm and 7.15 ppm integrating for 8, 8, 8, 8 protons each, making a total of 32 protons expected for mercaptopyridine protons and a singlet for phthalocyanine ring at 8.93 ppm intergrading for 8 protons.

The NMR spectra of the quaternized tetra-substituted phthalocyanine complex (**8**) showed more unresolved patterns compared to non-quaternized derivative. This complex showed the phthalocyanine ring protons and mercaptopyridine group protons as unresolved multiplets integrating for a total of 28 protons. Phthalocyanine ring and mercaptopyridine protons were observed between 9.74 and 6.91 ppm as multiplets. The methyl protons which integrated for 12 protons were observed at 4.33 ppm for complex **8** as a doublet due to the mixture of isomers. The NMR spectra of the quaternized octasubstituted phthalocyanine complex (**9**) showed more resolved patterns compared to quaternized tetra-substituted derivative (**8**). This complex (**9**) showed phthalocyanine ring protons at 9.14 ppm as a singlet integrating for 8 protons. Broad peaks at 10.13 ppm and 8.25 ppm, and a multiplet between 7.91 and 7.88 ppm, integrating for 4, 12, 16 protons each, making a total of 32 protons, belong to mercaptopyridine protons for **9**. The methyl protons which integrated for 24 protons were observed as a singlet at 4.51 ppm for complex **9**.

In addition to the elemental analysis results, the mass spectral data for the newly synthesized tetra- and octasubstituted zinc phthalocyanines (**5**,**6** and **8**,**9**) were consistent with the assigned formulations. The mass spectra of compounds were obtained by Electron Spray Ionization (ESI) technique for non-ionic complexes (**5**,**6**) and MALDI-TOF-MS for quaternized complexes (**8**,**9**). The molecular ion peaks of non-quaternized complexes showing parent ions were found at *m/z* 1013.2 $[M + H]^+$ for complex **5** and 1451.2 $[M + H]^+$ for complex **6**. The molecular ion peaks of quaternized complex **8** showed parent ions at *m/z* 1167 $[M-SO_4]^+$, 1073.6 $[M-2SO_4]^+$ 1042.1, $[M-2SO_4-2CH_3]^+$. MALDI-TOF-MS spectra of quaternized phthalocyanine complex (**8**) show the base peak cleavage of anion and methyl groups, as it is often observed for this type of compounds [51]. The molecular ion peaks for quaternized complex **9** was not observed.

3.2. Ground state electronic absorption and fluorescence spectra

The electronic spectra of the studied non-ionic (**5**–**7**) and quaternized ionic (**8**–**10**) zinc Pc complexes showed characteristic absorption in the Q band region at around 685–707 for complexes **5**–**7** and 685–704 nm for complexes **8**–**10** in DMSO, Table 1. The B bands were observed at around 320–370 nm in DMSO (Fig. 1a and b). The spectra showed monomeric behavior evidenced by a single (narrow) Q band which is typical of metallated phthalocyanine complexes in DMSO [52]. The Q bands of the non-peripherally substituted complexes (**5** and **8**) are red-shifted when compared to the corresponding peripherally substituted complexes (**7** and **10**) in DMSO (Fig. 1a and b). The red-shifts are observed 15 nm between **5** and **7**, and 6 nm between **8** and **10**. The observed red spectral shifts are typical of Pcs with substituents at the non-peripheral positions and have been explained in the literature [53,54]. The red-shift was observed for octa-peripherally substituted complex (**6**) compared to tetra-peripherally substituted complex (**7**) due to increase in the number of 2-mercaptopyridine groups which increase the electron donation due to sulfur atoms on the phthalocyanine framework for octa substitution. In water, the absorption spectra of quaternized complexes (**8**–**10**) showed cofacial aggregation, as evidenced by the presence of two non-vibrational peaks in the Q band region, Fig. 1c and d, Table 1. The lower energy (red-shifted) bands at 666 for **8**, 694 for **9** and 665 nm for **10** are due to the monomeric specie, while the higher energy (blue-shifted) bands at 636 for **8**, 656 for **9** and 630 nm for **10** are due to aggregated specie.

Aggregation is usually depicted as a coplanar association of rings progressing from monomer to dimer and higher order complexes. It is dependent on the concentration, nature of the solvent, nature of the substituents, complexed metal ions and temperature [55]. In the aggregated state the electronic structure of the complexed phthalocyanine rings are perturbed resulting in alternation of the ground and excited state electronic structures [56]. In this study, the aggregation behavior of the Pc complexes (**5**–**7** and **8**–**10**) was investigated at different concentrations in DMSO (Fig. 2, for complex **9** as an example). The Beer–Lambert law was obeyed for all of these complexes at concentrations ranging from 1.2×10^{-5} to 4×10^{-6} M. The studied zinc Pc complexes (**5**–**7** and **8**–**10**) did not show aggregation in DMSO.

Fig. 3 shows fluorescence emission, absorption and excitation spectra of complex **5** in DMSO as example of the studied zinc Pc complexes. Fluorescence emission peaks are listed in Table 1. The observed Stokes shifts were within the region (~10–20 nm) observed for zinc Pc complexes. All studied zinc Pc complexes (**5**–**10**) showed similar fluorescence behavior in DMSO. The excitation spectra were similar to absorption spectra and both were mirror images of the fluorescent spectra for all zinc Pc complexes in DMSO. The proximity of the wavelength of each component of the Q band absorption to the Q band maxima of the excitation spectra for all zinc Pc complexes suggested that the nuclear configurations of the ground and excited states are similar and not affected by

Table 1
Absorption, excitation and emission spectral data for unsubstituted, tetra- and octasubstituted zinc phthalocyanine complexes in DMSO and water.

Compound	Solvent	Q band λ_{max}, (nm)	(log ϵ)	Excitation λ_{Ex}, (nm)	Emission λ_{Em}, (nm)	Stokes shift Δ_{Stokes}, (nm)
5	DMSO	700	5.21	701	717	17
6	DMSO	707	5.14	710	721	14
7	DMSO	685[a]	5.38	686[a]	698[a]	12[a]
8	DMSO	691	5.03	692	707	16
	H_2O	636, 666	4.67, 4.68	–	–	–
9	DMSO	704	5.22	706	716	12
	H_2O	656, 694	4.48, 4.32	695	707	13
10	DMSO	685[a]	4.96	687[a]	698[a]	11[a]
	H_2O	630, 665[a]	4.50, 4.51	–	–	–
ZnPc	DMSO	672[b]	5.38	672[b]	681[b]	9[b]

[a] Data from reference [33].
[b] Data from reference [70].

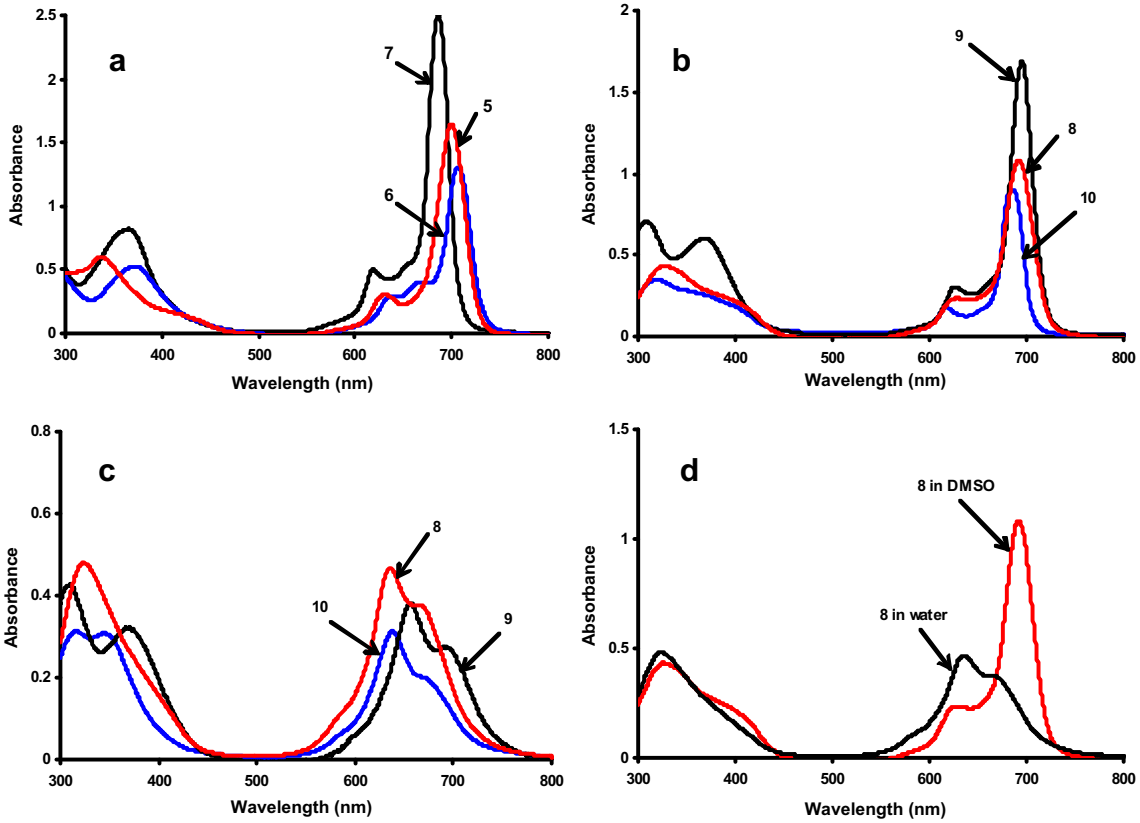

Fig. 1. Absorption spectra of: (a) substituted non-ionic zinc Pc complexes **(5–7)** in DMSO, (b) substituted quaternized ionic zinc Pc complexes **(8–10)** in DMSO and (c) water, (d) substituted quaternized ionic zinc Pc complex **8** in DMSO and water. Concentration = 1×10^{-5} M.

excitation. In aqueous media, the water-soluble quaternized zinc Pc complexes (**8–10**) are not fluorescent. Aggregated MPc complexes are not known to fluorescence [57] since aggregation lowers the photoactivity of molecules through dissipation of energy.

3.3. Fluorescence quantum yields and lifetimes

The fluorescence quantum yields (Φ_F) for non-ionic zinc Pc complexes (**5–7**) in DMSO and for quaternized ionic complexes (**8–10**) in both DMSO and water are given in Table 2. The Φ_F values of the studied zinc Pc complexes (**5–7** and **8–10**) are slightly lower than unsubstituted zinc Pc in DMSO, suggesting that more quenching of substitution of the 2-mercaptopyridine groups on the Pc framework. The Φ_F values of non-ionic zinc Pc complexes are similar and typical MPc complexes in DMSO [57]. The peripherally tetra-substituted complex (**7**) shows largest Φ_F value in DMSO compared to the others complexes, Table 2. The non-ionic zinc Pc complexes (**5–7**) show larger Φ_F values compared to the corresponding quaternarized ionic zinc Pc complexes (**8–10**) in DMSO. Comparing DMSO and water, while the quaternarized ionic zinc Pc complexes (**8–10**) are fluorescent in DMSO, these complexes are

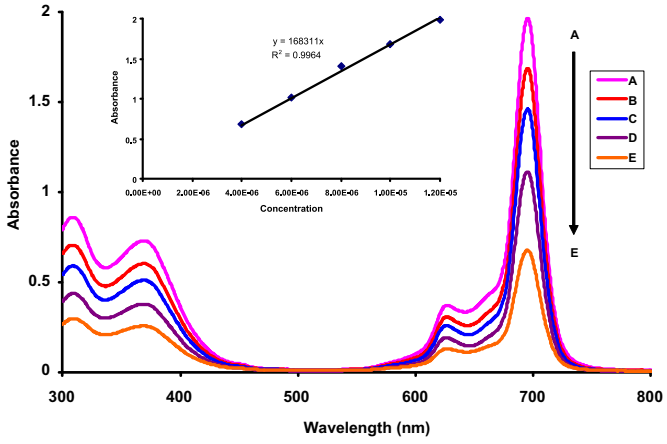

Fig. 2. Aggregation behavior of **9** in DMSO at different concentrations: 12×10^{-6} (A), 10×10^{-6} (B), 8×10^{-6} (C), 6×10^{-6} (D), 4×10^{-6} (E) M. (Inset: Plot of absorbance versus concentration).

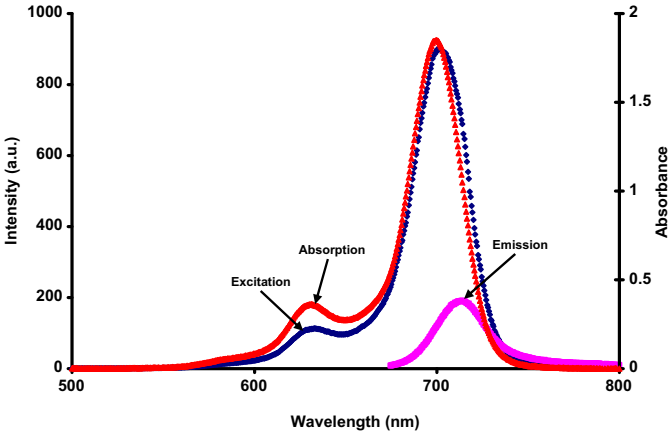

Fig. 3. Absorption, excitation and emission spectra of **5** in DMSO. Excitation wavelength: 665 nm.

Table 2
Photophysical and photochemical parameters of unsubstituted, tetra- and octa-substituted zinc phthalocyanine complexes in DMSO and water.

Compound	Solvent	Φ_F	τ_F (ns)	k_F (s^{-1}) ($\times 10^8$)[a]	τ_0 (ns)	Φ_d ($\times 10^{-5}$)	Φ_Δ
5	DMSO	0.12	0.92	1.31	7.65	1.87	0.57
6	DMSO	0.11	1.10	1.00	10.00	2.19	0.51
7	DMSO	0.17	1.20	1.58	6.34	0.66	0.86[b]
8	DMSO	0.01	0.19	0.75	13.35	2.64	0.45
	H_2O	–	–	–	–	2.30	0.19
9	DMSO	0.03	0.17	1.70	5.88	10.58	0.63
	H_2O	–	–	–	–	3.61	0.10
10	DMSO	0.02[b]	0.20[b]	0.66	15.18	6.74	0.82[b]
	H_2O	–	–	–	–	2.04	0.45[b]
ZnPc	DMSO	0.20[c]	1.22[d]	1.47[d]	6.80[d]	2.61[d]	0.67[d]

[a] k_F is the rate constant for fluorescence. Values calculated using $k_F = \Phi_F/\tau_F$.
[b] Data from reference [33].
[c] Data from reference [37].
[d] Data from reference [70].

not fluorescent in water. This is attributed to aggregation as discussed above.

Fluorescence lifetime (τ_F) refers to the average time a molecule stays in its excited state before emission, and its value is directly related to that of Φ_F; i.e. the longer the lifetime, the higher the quantum yield of fluorescence. Any factor that shortens the fluorescence lifetime of a fluorophore indirectly reduces the value of Φ_F. Such factors include internal conversion and intersystem crossing. As a result, the nature and the environment of a fluorophore determine its fluorescence lifetime. Lifetimes of fluorescence were calculated using the Strickler–Berg equation. Using this equation, a good correlation has been found [36] between experimentally and the theoretically determined lifetimes for the unaggregated molecules as is the case for DMSO in this work. The τ_F value is higher for peripherally tetra-substituted zinc complex (**7**) when compared to non-peripherally tetra-substituted (**5**) and peripherally octasubstituted complex (**6**) in DMSO. For the quaternarized ionic complexes, the τ_F value is higher for peripheral complex (**10**) when compared to **9**, but the value for **10** is similar to the one for **8**, Table 2.

The natural radiative lifetime (τ_0) and the rate constants for fluorescence (k_F) values are also given in Table 2. But there was no clear trend found for τ_0 and k_F values among the studied zinc Pc complexes.

3.4. Singlet oxygen quantum yields

Energy transfer between the triplet state of photosensitizers and ground state molecular oxygen leads to the production of singlet oxygen. There is a necessity of high efficiency of transfer of energy between excited triplet state of MPc and ground state of oxygen to generate large amounts of singlet oxygen, essential for PDT. The singlet oxygen quantum yields (Φ_Δ), give an indication of the potential of the complexes as photosensitizers in applications where singlet oxygen is required, (e.g. for Type II mechanism). The Φ_Δ values were determined using a chemical method (using DPBF in DMSO and ADMA in water as quenchers). The disappearance of DPBF or ADMA was monitored using UV–vis spectrophotometer (Fig. 4a using DPBF in DMSO and Fig. 4b using ADMA in water for complex **9**). Many factors are responsible for the magnitude of the determined quantum yield of singlet oxygen including; triplet excited state energy, ability of substituents and solvents to quench the singlet oxygen, the triplet excited state lifetime and the efficiency of the energy transfer between the triplet excited state and the ground state of oxygen. There was no decrease in the Q band of formation of the ZnPc derivatives during Φ_Δ determinations (Fig. 4).

Table 2 shows that while the Φ_Δ values are higher for peripherally tetra-substituted zinc Pc complexes (**7** and **10**) in DMSO, the Φ_Δ values of the non-peripherally tetra-(**5** and **8**) and peripherally octa-(**6** and **9**) substituted zinc Pc derivatives are lower when compared to respective unsubstituted zinc Pc. The peripherally tetra-substituted complexes (**7** and **10**) showed higher Φ_Δ values when compared to the non-peripherally tetra-(**5** and **8**) and peripherally octa-(**6** and **9**) substituted zinc Pc complexes in DMSO. Quaternarized ionic zinc Pc complexes (**8**–**10**) showed lower Φ_Δ values when compared to corresponding non-ionic complexes (**5**–**7**) in DMSO, suggesting that the quaternization of the zinc Pc complexes caused the decrease in the Φ_Δ values. Table 2 shows that lower Φ_Δ values are observed in aqueous solutions compared to in DMSO. The low Φ_Δ in water compared to other solvents such as deuterated water and DMSO was explained [37] by the fact that singlet oxygen absorbs at 1270 nm, and water, which absorbs around this wavelength has a great effect on singlet oxygen lifetime, while DMSO which exhibits little absorption in this region has longer singlet oxygen lifetimes than water, resulting in larger Φ_Δ values in DMSO. The quaternized peripherally tetra-substituted zinc Pc complex (**10**) showed highest Φ_Δ value than other studied quaternized zinc Pc complexes in water.

Singlet oxygen quantum yield (Φ_Δ) values of all employed mercaptopyridine substituted zinc Pc complexes were higher (ranging from 0.51–0.86 in DMSO), than those of their corresponding pyridyloxy substituted zinc Pc complexes in literature that ranged from 0.06–0.46 [51,58]. The Φ_Δ values, found in this study, are similar to those of Cd(II), Hg(II), Ga(III), In(III), Si(IV) and

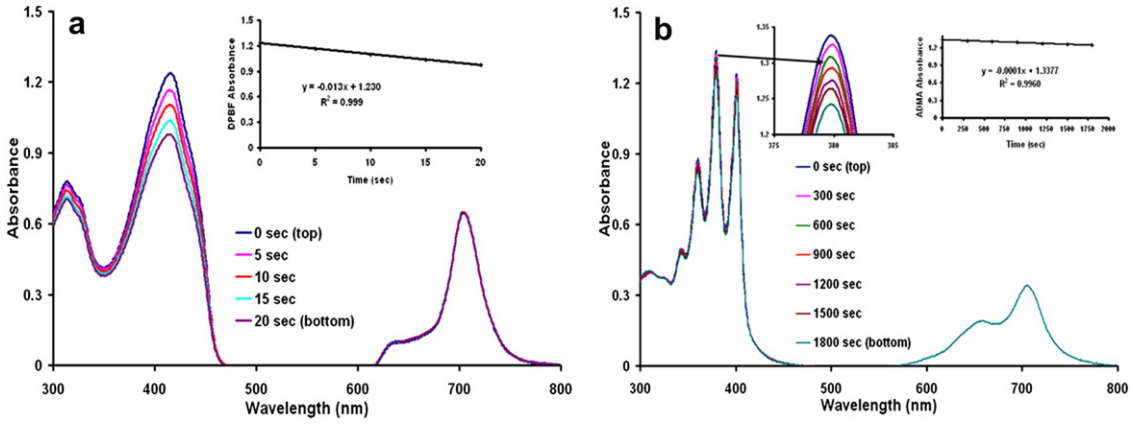

Fig. 4. A typical spectrum for the determination of singlet oxygen quantum yield of: (a) **9** in DMSO using DPBF as a singlet oxygen quencher and (b) **9** in water using ADMA as a singlet oxygen quencher. Concentration = 1×10^{-5} M (Inset: Plots of DPBF or ADMA absorbance versus time).

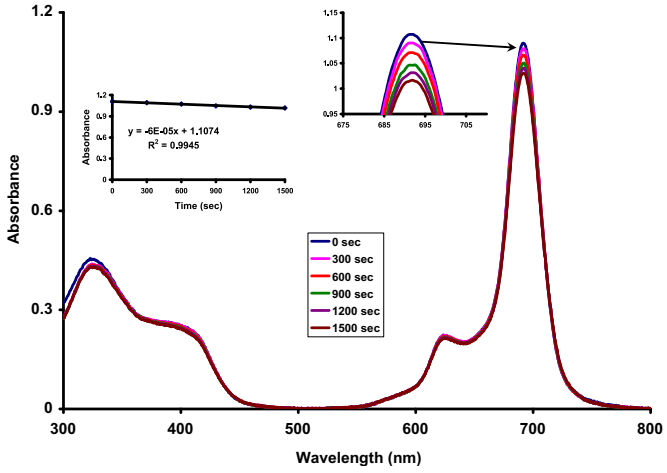

Fig. 5. The photodegradation of **8** in DMSO showing the disappearance of the Q band at 5 min intervals. (Inset: Plot of Q band absorbance versus time).

Sn(IV) Pc complexes having pyridyloxy or mercaptopyridine groups on the phthalocyanine ring reported in literature [16,51,58–64]. The peripheral tetra-2-mercaptopyridine substituted zinc Pc complexes (**7** and **10**), studied in this work gave highest Φ_Δ values (0.86 for complex **7** in DMSO and 0.45 for complex **10** in water), compared to 2-mercaptopyridine substituted Pc complexes in literature [60,62]. A value of $\Phi_\Delta = 0.86$ is the highest ever reported for a ZnPc derivative.

3.5. Photodegradation studies

Degradation of the molecules under irradiation can be used to study their stability and this is especially important for those molecules intended for use in photocatalysis. The collapse of the absorption spectra without any distortion of the shape confirms clean photodegradation not associated with phototransformation into different forms of MPc absorbing in the visible region. The spectral changes observed for all the complexes (**5**–**7** and **8**–**10**) during confirmed photodegradation occurred without photo-transformation (Fig. 5 as an example for complex **8** in DMSO).

All the studied zinc Pc complexes showed about the same stability with Φ_d of the order of 10^{-5}. The Φ_d values, found in this study, are similar with zinc Pc complexes having different substituents on the phthalocyanine ring in the literature [57]. Stable zinc phthalocyanine complexes show Φ_d values as low as 10^{-6} and for

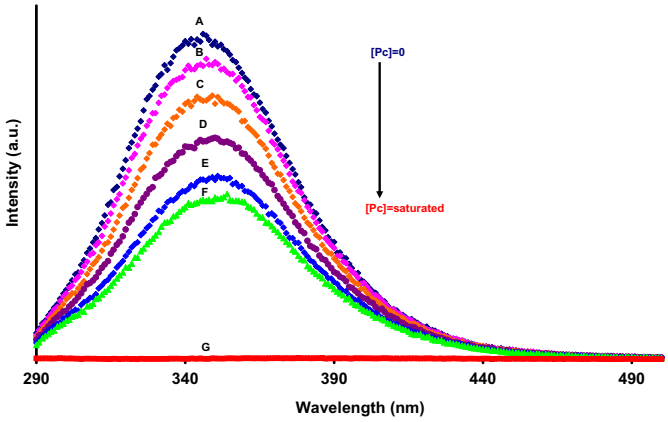

Fig. 6. Fluorescence emission spectral changes of BSA ($C = 3.00 \times 10^{-5}$ M) on addition of varying concentrations of **8** in water [8].: $A = 0$, $B = 1.66 \times 10^{-6}$, $C = 3.33 \times 10^{-6}$, $D = 5.00 \times 10^{-6}$, $E = 6.66 \times 10^{-6}$, $F = 8.33 \times 10^{-6}$ M, G = saturated with **8**.

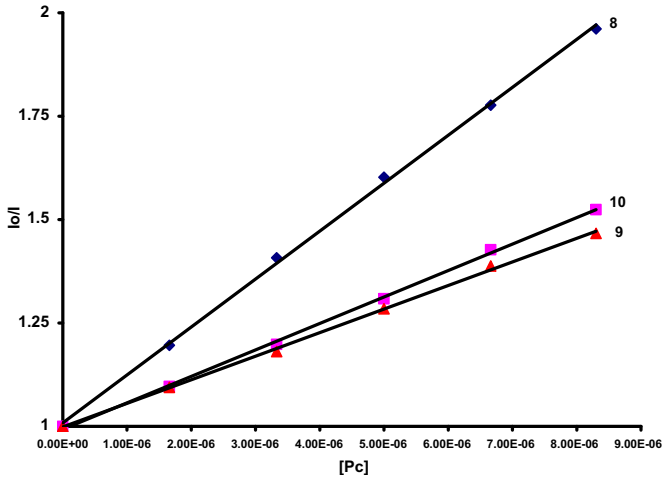

Fig. 7. Stern–Volmer plots of 2-mercaptopyridine substituted zinc phthalocyanines quenching of BSA in water. [BSA] = 3.00×10^{-5} M in water. [Pc] = 0, 1.66×10^{-6}, 3.33×10^{-6}, 5.00×10^{-6}, 6.66×10^{-6}, 8.33×10^{-6} M.

unstable molecules, values of the order of 10^{-3} have been reported [57]. The non-ionic zinc Pc complexes (**5**–**7**) showed lower Φ_d values when compared to the unsubstituted ZnPc in DMSO, whereas, the ionic zinc Pc complexes (**8**–**10**) showed higher Φ_d values (compared to **5**–**7**), suggesting that the substitution of the 2-mercaptopyridine groups on the phthalocyanine framework increasing the stability of the zinc Pc complexes, but the quaternization of these groups resulted in the decrease in the stability of the ionic zinc Pc complexes.

3.6. Binding of quaternized zinc phthalocyanine complexes to BSA

Fig. 6 shows the changes in the fluorescence emission spectra of BSA in the presence of different concentrations of **8** (as an example) in water. The quaternized ionic zinc Pc complexes are mixtures of aggregated and unaggregated species. The total concentrations of the complexes are mixture of the monomer and aggregated species. We calculated the percentage aggregation (% Agg) of these complexes using the equation described in the literature [65,66]. The aggregation percentages are 3.7% for **8**, 28.3% for **10** and 6.4% for **9** in water. The non-peripherally substituted Pc complex showed lowest percentage aggregation value, probably due to reduced aggregation tendencies when substitution is at the non-peripheral position of the Pc skeleton [67]. The BSA fluorescence at 348 nm is mainly attributable to tryptophan residues in the macromolecule. BSA and the respective quaternized ionic Pc complexes exhibit reciprocated fluorescence quenching on one another; hence it was possible to determine Stern–Volmer quenching constants (K_{SV}). The slope of the plots shown at Fig. 7 gave K_{SV} values which are listed in Table 3. These values suggest that BSA fluorescence quenching is more effective for quaternized non-peripherally substituted Pc complex (**8**) than quaternized peripherally substituted Pc complex (**10**) and octasubstituted Pc complex (**9**) in water. Using the approximate fluorescence lifetime of BSA [48,49],

Table 3
Binding and fluorescence quenching data for interaction of BSA with quaternized ionic zinc phthalocyanine complexes in water.

Compound	$K_{SV}^{BSA}/10^5$ (M^{-1})	$k_q/10^{13}$ (M^{-1} s^{-1})	$K_b/10^{-6}$ (M^{-1})	n
8	1.16	1.16	8.13	1.56
9	0.55	0.55	15.14	1.48
10	0.65	0.65	10.96	1.58

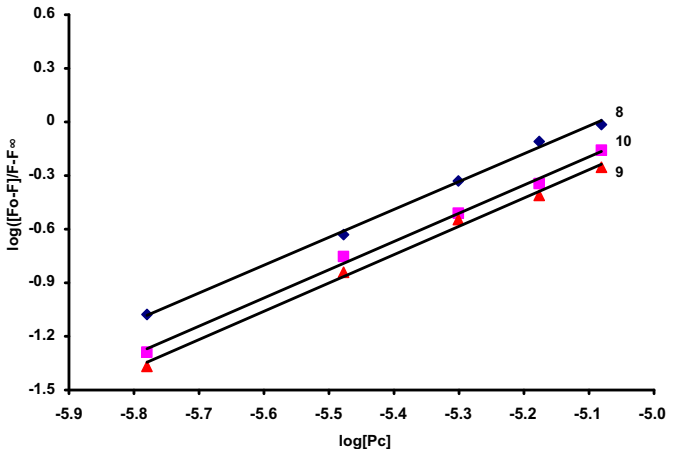

Fig. 8. Determination of 2-mercaptopyridine substituted zinc phthalocyanine-BSA binding constant (and number of binding sites on BSA). [BSA] = 3.00×10^{-5} M and [Pc] = 0, 1.66×10^{-6}, 3.33×10^{-6}, 5.00×10^{-6}, 6.66×10^{-6}, 8.33×10^{-6} M in water.

the bimolecular quenching constant (k_q) was determined using equation (7). These values are of the order of 10^{13} M^{-1} s^{-1}, which exceed the proposed value of 10^{10} M^{-1} s^{-1} for diffusion-controlled (dynamic) quenching (according to the Einstein-Smoluchowski approximation) at room temperature [68]. This also, is an indication that the mechanism of BSA quenching by quaternized Pc complexes (**8**, **9** and **10**) is not diffusion-controlled (i.e., not dynamic quenching, but static quenching). The k_q value is larger for quaternized non-peripherally substituted Pc complex (**8**) than quaternized peripherally tetra-(**10**) and octa-(**9**) substituted zinc Pc complexes in water. The binding constants (K_b) and number of binding sites (n) on BSA were obtained using Eq. (5) and the results are shown in Table 3. The slope of the plots shown at Fig. 8 gave n values and the intercepts of these plots gave K_b values. The values of K_b and n are typical of MPc-BSA interactions in aqueous solutions [45,69]. The higher K_b value for quaternized peripherally octasubstituted Pc complex (**9**) implies that a peripherally octasubstituted zinc Pc complex binds more strongly to BSA than the other quaternized zinc Pc (**8** and **10**). The decrease in the intrinsic fluorescence intensity of tryptophan with quaternized Pc concentration indicates that these complexes readily bind to BSA, which implies that the Pc molecules reach subdomains where tryptophan residues are located in BSA. This also suggests that the primary binding sites of these molecules are very close to tryptophan residues, since the occurrence of quenching requires molecular contact.

4. Conclusion

The synthesis and characterization of non-peripherally tetra-(**5**) and peripherally octa-(**6**) substituted zinc Pc complexes and their quaternized derivatives (**8** and **9**) have been undertaken. The spectral, photophysical and photochemical properties of non-peripherally tetra-, peripherally tetra- and peripherally octa-2-mercaptopyridine substituted non-ionic (**5-7**) and quaternized ionic (**8**–**10**) zinc Pc complexes are compared. The effects of the number and position of the substituents, quaternization of the 2-mercaptopyridine groups and the solvents (DMSO or water for ionic complexes) on the properties of the zinc Pc complexes are also presented. All studied zinc Pc complexes did not show aggregation in DMSO. The quaternized complexes exhibited excellent solubility in water, but they showed aggregation in this solvent. Although, the photophysical and photochemical properties relevant for photosensitization gave more attractive values in DMSO, the values in water are still good enough for PDT applications. These complexes gave good Φ_Δ values. In particular, quaternarized peripheral zinc Pc complex (**10**) has high Φ_Δ value (0.45) in water. Thus, these complexes exhibit potential as Type II photosensitizers for PDT of cancer. This work will certainly enrich the hitherto scanty literature on the potentials of cationic zinc phthalocyanines as photosensitizers in PDT. This study reveals that the water-soluble complexes bind strongly to serum albumin; hence they can easily be transported in the blood.

Acknowledgements

This work was supported by the Department of Science and Technology (DST) and National Research Foundation (NRF), South Africa through DST/NRF South African Research Chairs Initiative for Professor of Medicinal Chemistry and Nanotechnology as well as Rhodes University and Medical Research Council of South Africa and Scientific Research Project of Gebze Institute of Technology (BAP-2007-A-01).

References

[1] Kadish K, Smith KM, Guilard R, editors. The porphyrin handbook, Vols. 15–20. Boston: Academic Press; 2003.
[2] Leznoff CC, Lever ABP. In: Phthalocyanines: properties and applications, Vols. 1–4. New York: VCH Publishers; 1989–1996.
[3] McKeown NB. Phthalocyanine materials. Cambridge: Cambridge University Press; 1998.
[4] Gregory P. Industrial applications of phthalocyanines. Journal of Porphyrins and Phthalocyanines 2000;4:432–7.
[5] Daimon K, Nukada K, Sakaguchi Y, Igarashi R. A new polymorph of hydroxygallium phthalocyanine and its application in a photoreceptor. The Journal of Imaging Science and Technology 1996;40:249–53.
[6] Tracz A, Makowski T, Masirek S, Pisula W, Geerts YH. Macroscopically aligned films of discotic phthalocyanine by zone casting. Nanotechnology 2007;18:485303.
[7] Priola SA, Raines A, Caughey WS. Porphyrin and phthalocyanine antiscrapie compounds. Science 2000;287:1503–606.
[8] Ben-Hur E, Chan WS. In: Kadish K, Smith KM, Guilard R, editors. The porphyrin handbook, vol. 19. Boston: Academic Press; 2003. p. 1–35.
[9] Ben-Hur E, Green M, Prager A, Kol R, Rosenthal I. Phthalocyanine photosensitization of mammalian cells: biochemical and ultrastructural effects. Photochemistry and Photobiology 1987;46:651–6.
[10] MacDonald IJ, Dougherty TJ. Basic principles of photodynamic therapy. Journal of Porphyrins Phthalocyanines 2001;5:105–29.
[11] Ali H, van Lier JE. Metal complexes as photo- and radiosensitizers. Chemical Reviews 1999;99:2379–450.
[12] Bonnett R. Photosensitizers of the porphyrin and phthalocyanine series for photodynamic therapy. Chemical Society Reviews 1995;24:19–33.
[13] Tedesco AC, Rotta JCG, Lunardi CN. Synthesis, photophysical and photochemical aspects of phthalocyanines for photodynamic therapy. Current Organic Chemistry 2003;7:187–96.
[14] Dumoulin F, Durmuş M, Ahsen V, Nyokong T. Synthetic pathways to water-soluble phthalocyanines. Coordination Chemistry Reviews 2010;254:2792–847.
[15] Karaoğlan GK, Gümrükçü G, Koca A, Gül A. The synthesis, characterization, electrochemical and spectroelectrochemical properties of a novel, cationic, water-soluble Zn phthalocyanine with extended conjugation. Dyes and Pigments 2011;88:247–56.
[16] Masilela N, Nyokong T. The synthesis and photophysical properties of water soluble tetrasulfonated, octacarboxylated and quaternised 2,(3)-tetra-(2-pyridiloxy) Ga phthalocyanines. Dyes and Pigments 2010;84:242–8.
[17] BŞ Sesalan, Koca A, Gül A. Water soluble novel phthalocyanines containing dodeca-amino groups. Dyes and Pigments 2008;79:259–64.
[18] Zimcik P, Miletin M, Musil Z, Kopecky K, Kubza L, Brault D. Cationic azaphthalocyanines bearing aliphatic tertiary amino substituents—Synthesis, singlet oxygen production and spectroscopic studies. Journal of Photochemistry and Photobiology A: Chemistry 2006;183:59–69.
[19] Filippis MP, Dei D, Fantetti L, Roncucci G. Synthesis of a new water-soluble octa-cationic phthalocyanine derivative for PDT. Tetrahedron Letters 2000;41:9143–7.
[20] Scalise I, Durantini EN. Synthesis, properties, and photodynamic inactivation of *Escherichia coli* using a cationic and a noncharged Zn(II) pyridyloxyphthalocyanine derivatives. Bioorganic & Medicinal Chemistry 2005;13:3037–45.
[21] Wood SR, Holroyd JA, Brown SB. The subcellular localization of Zn(II) phthalocyanines and their redistribution on exposure to light. Photochemistry and Photobiology 1997;65:397–402.

[22] Castano AP, Demidova TN, Hamblin MR. Mechanisms in photodynamic therapy: part one-photosensitizers, photochemistry and cellular localization. Photodiagnosis and Photodynamic Therapy 2004;1:279–93.
[23] Gürek AG, Durmuş M, Ahsen V. Synthesis and mesomorphic properties of tetra- and octa-substituted phthalocyanines. New Journal of Chemistry 2004; 28:693–9.
[24] Atilla D, Durmuş M, Gürek AG, Ahsen V, Nyokong T. Synthesis, photophysical and photochemical properties of poly(oxyethylene)-substituted zinc phthalocyanines. Dalton Transactions; 2007:1235–43.
[25] Yuksel F, Durmus M, Ahsen V. Photophysical, photochemical and liquid crystalline properties of novel gallium (III) phthalocyanines. Dyes and Pigments 2011;90:191–200.
[26] Atilla D, Gürek AG, Basova TV, Kiselev VG, Hassan A, Sheludyakova LA, et al. The synthesis and characterization of novel mesomorphic octa- and tetra-alkylthio-substituted lead phthalocyanines and their films. Dyes and Pigments 2011;88:280–9.
[27] Carter DC, Ho JX. Structure of serum albumin. Advances in Protein Chemistry 1994;45:153–76.
[28] Peters T. Serum albumin. Advances in Protein Chemistry 1985;37:161–245.
[29] Perrin DD, Armarego WLF. Purification of laboratory chemicals. 2nd ed. Oxford: Pegamon Press; 1989.
[30] George RD, Snow AW. Synthesis of 3-nitrophthalonitrile and tetra-α-substituted phthalocyanines. Journal of Heterocyclic Chemistry 1995;32:495–8.
[31] Wöhrle D, Eskes M, Shigehara K, Yamada A. A Simple Synthesis of 4,5-disubstituted benzenes and octasubstituted phthalocyanines. Synthesis; 1993:194–6.
[32] Sehlotho N, Durmuş M, Ahsen V, Nyokong T. The synthesis and electrochemical behaviour of water soluble manganese phthalocyanines: anion radical versus Mn(I) species. Inorganic Chemistry Communication 2008;11: 479–83.
[33] Saydan N, Durmuş M, Dizge MG, Yaman H, Gürek AG, Antunes E, et al. Water-soluble phthalocyanines mediated photodynamic effect on mesothelioma cells. Journal of Porphyrins and Phthalocyanines 2009;13:681–90.
[34] Ogunsipe A, Nyokong T. Photophysical and photochemical studies of sulphonated non-transition metal phthalocyanines in aqueous and non-aqueous media. Journal of Photochemistry and Photobiology A: Chemistry 2005; 173:211–20.
[35] Fery-Forgues S, Lavabre D. Are fluorescence quantum yields so tricky to measure? A demonstration using familiar stationery products. Journal of Chemical Education 1999;76:1260–4.
[36] Maree D, Nyokong T, Suhling K, Phillips D. Effects of axial ligands on the photophysical properties of silicon octaphenoxyphthalocyanine. Journal of Porphyrins and Phthalocyanines 2002;6:373–6.
[37] Ogunsipe A, Chen JY, Nyokong T. Photophysical and photochemical studies of zinc(II) phthalocyanine derivatives—effects of substituents and solvents. New Journal of Chemistry 2004;28:822–7.
[38] Du H, Fuh RA, Li J, Corkan A, Lindsey JS. PhotochemCAD: a computer-aided design and research tool in photochemistry. Photochemistry and Photobiology 1998;68:141–2.
[39] Brannon JH, Madge D. Picosecond laser photophysics. Group 3A phthalocyanines. Journal of the American Chemical Society 1980;102:62–5.
[40] Seotsanyana-Mokhosi I, Kuznetsova N, Nyokong T. Photochemical studies of tetra-2,3-pyridinoporphyrazines. Journal of Photochemistry and Photobiology A: Chemistry 2001;140:215–22.
[41] Kuznetsova N, Gretsova N, Kalmkova E, Makarova E, Dashkevich S, Negrimovskii V, et al. Relationship between the photochemical properties and structure of porphyrins and related compounds. Russian Journal of General Chemistry 2000;70:133–40.
[42] Wilkinson F, Helman WP, Ross AB. Quantum yields for the photosensitized formation of the lowest electronically excited singlet state of molecular oxygen in solution. Journal of Physical and Chemical Reference Data 1993;22:113–262.
[43] Spiller W, Kliesch H, Wöhrle D, Hackbarth S, Roder B, Schnurpfeil G. Singlet oxygen quantum yields of different photosensitizers in polar solvents and micellar solutions. Journal of Porphyrins and Phthalocyanines 1998;2:145–58.
[44] Chipman DM, Grisaro V, Shanon N. The binding of oligosaccharides containing n-acetylglucosamine and n-acetylmuramic acid to lysozyme: the specificity of binding subsites. The Journal of Biological Chemistry 1967;242:4388–94.
[45] Nunes SMT, Sguilla FS, Tedesco AC. Photophysical studies of zinc phthalocyanine and chloroaluminum phthalocyanine incorporated into liposomes in the presence of additives. Brazilian Journal of Medical and Biological Research 2004;37:273–84.
[46] Lehrer S, Fashman GD. The fluorescence of lysozyme and lysozyme substrate complexes. Biochemical and Biophysical Research Communications 1966; 23:133–8.
[47] Lakowicz JR, Weber G. Quenching of fluorescence by oxygen. Probe for structural fluctuations in macromolecules. Biochemistry 1973;12:4161–70.
[48] Jiang CQ, Gao MX, He JX. Study of the interaction between terazosin and serum albumin: synchronous fluorescence determination of terazosin. Analytica Chimica Acta 2002;452:185–9.
[49] Gou M, Zou JW, Yi PG, Shang ZC, Hu GX, Yu QS. Binding interaction of gatifloxacin with bovine serum albumin. Analytical Sciences 2004;20:465–70.
[50] Leznoff CC. In: Leznoff CC, Lever ABP, editors. Phthalocyanines: properties and applications, Vol. 1. New York: VCH Publishers; 1989 [Chapter 1].
[51] Li H, Jensen TJ, Fronczek FR, Vicente MGH. Syntheses and properties of a series of cationic water-soluble phthalocyanines. Journal of Medicinal Chemistry 2008;51:502–11.
[52] Stillman MJ, Nyokong T. In: Leznoff CC, Lever ABP, editors. Phthalocyanines: properties and applications, Vol. 1. New York: VCH Publishers; 1989 [Chapter 3].
[53] Anderson AB, Gorden TL, Kenney ME. Electronic and redox properties of stacked-ring silicon phthalocyanines from molecular orbital theory. Journal of the American Chemical Society 1985;107:192–5.
[54] Konami M, Hatano M, Tajiri A. Inter-ring overlap integrals in dimer complexes of phthalocyanines and porphyrins. Chemical Physics Letters 1990; 166:605–8.
[55] Enkelkamp H, Nolte RJM. Molecular materials based on crown ether functionalized phthalocyanines. Journal of Porphyrins and Phthalocyanines 2000;4:454–9.
[56] Dominquez DD, Snow AW, Shirk JS, Pong RGS. Polyethyleneoxide-capped phthalocyanines: limiting phthalocyanine aggregation to dimer formation. Journal of Porphyrins and Phthalocyanines 2001;5:582–92.
[57] Nyokong T. Effects of substituents on the photochemical and photophysical properties of main group metal phthalocyanines. Coordination Chemistry Reviews 2007;251:1707–22.
[58] Chidawanyika W, Ogunsipe Nyokong T. Syntheses and photophysics of new phthalocyanine derivatives of zinc, cadmium and mercury. New Journal of Chemistry 2007;31:377–84.
[59] Durmuş M, Nyokong T. The synthesis, fluorescence behaviour and singlet oxygen studies of new water-soluble cationic gallium(III) phthalocyanines. Inorganic Chemistry Communications 2007;10:332–8.
[60] Moeno S, Nyokong T. Solvent and central metal effects on the photophysical and photochemical properties of peripherally tetra mercaptopyridine substituted metallophthalocyanines. Journal of Photochemistry and Photobiology A: Chemistry 2009;203:204–10.
[61] Durmuş M, Nyokong T. Synthesis, photophysical and photochemical studies of new water-soluble indium(III) phthalocyanines. Photochemical and Photobiological Science 2007;6:659–68.
[62] Durmuş M, Ahsen V. Water-soluble cationic gallium(III) and indium(III) phthalocyanines for photodynamic therapy. Journal of Inorganic Biochemistry 2010;104:297–309.
[63] Ogunsipe A, Nyokong T, Durmuş M. Photophysical, photochemical and bovine serum albumin binding studies on water-soluble gallium(III) phthalocyanine derivatives. Journal of Porphyrins Phthalocyanines 2007;11:635–44.
[64] Durmuş M, Erdoğmuş A, Ogunsipe A, Nyokong T. The synthesis and photophysicochemical behaviour of novel water-soluble cationic indium(III) phthalocyanine. Dyes and Pigments 2009;82:244–50.
[65] Idowu M, Nyokong T. Photophysical and photochemical properties of tetrasulfonated silicon and germanium phthalocyanine in aqueous and non-aqueous media. Journal of Photochemistry and Photobiology A: Chemistry 2008;197:273–80.
[66] Khene S, Ogunsipe A, Antunes E, Nyokong T. Microwave synthesis and photophysics of new tetrasulfonated tin(II) macrocycles. Journal of Porphyrins and Phthalocyanines 2007;11:109–17.
[67] George RD, Snow AW, Shirk JS, Barger WR. The Alpha substitution effect on phthalocyanine aggregation. Journal of Porphyrins and Phthalocyanines 1998;2:1–7.
[68] Murov SL, Carmichael I, Hug GL. Handbook of photochemistry. 2nd ed. New York: M. Decker; 1993.
[69] Nilsson R, Kearns DR. Role of singlet oxygen in some chemiluminescence and enzyme oxidation reactions. The Journal of Physical Chemistry 1974;78:1681–3.
[70] Gürol I, Durmuş M, Ahsen V, Nyokong T. Synthesis, photophysical and photochemical properties of substituted zinc phthalocyanines. Dalton Transactions; 2007:3782–91.